Failure criteria for single crystal alloys of gas turbine blades under static and thermocyclic loading

Getsov L.B. [1,a], Semenov A.S. [2,b], Tikhomirova E.A. [3] and Rybnikov A.I. [1]

[1] NPO ZKTI, Russia

[2] St. Petersburg state polytechnical university, Russia

[3] Klimov Company, Russia

[a] Guetsov@yahoo.com, [b] Semenov.Artem@googlemail.com

Keywords: single crystal, gas turbine blade, thermo-mechanical fatigue, damage, crystallographic and non-crystallographic failure modes.

Abstract. The problem of thermo–mechanical fatigue (TMF) of single crystal turbine blades has not been fully investigated neither theoretically nor experimentally. In the present work TMF tests were performed for two single crystal nickel-based alloys with various crystallographic orientations (⟨001⟩, ⟨011⟩, ⟨111⟩) under different temperatures and cycle durations. The dependence of the failure modes (crystallographic or non-crystallographic) on loading regimes was analyzed. The nonlinear viscoelastic, elastoplastic and viscoelastoplastic material models with nonlinear kinematic hardening were used to predict the cyclic stress-strain state, ratcheting and creep of the samples. The deformation criterion of damage accumulation was introduced for the lifetime prediction. The stress analysis of single crystal samples with concentrators (in the form of circular holes) and without them was carried out with use of "physical" models of plasticity and creep. These material models take into account that the inelastic deformation occurs by a slip mechanism and is determined by the crystallographic orientation. The proposed failure model with using deformation criterion allows qualitatively and quantitatively to predict the TMF fracture process of single crystals.

Introduction

The widespread use of single crystal alloys for the manufacturing of blades of gas turbine engine allowing a significant increase in the gas temperature before turbine, sets a number of tasks, which should help increase the reliability of stress and strength analysis. In the present investigation the results of experimental studies of single-crystal nickel-based alloys, as well as approaches to the computation of the stress-strain state and strength of structural parts are considered and discussed.

Materials and methods of research

Experimental studies were performed on two single crystal alloys ZhS32 and ZhS36 with different alloying and, most importantly, different carbon contents and were designed to expand the information given in [1, 2]. The tests of mechanical properties, creep and thermal fatigue resistance at different temperatures were carried out.

The creep tests were conducted on the installation of ATS (U.S.) with determination of the kinetics of accumulated inelastic deformation at the first stage as well as at the steady state of creep.

Test methods for TMF are described in particular in [3]. For the tests rigidly clamped samples with a polished surface were used, as shown in Fig. 1. Tests were conducted in a vacuum that allows during the testing to observe the formation of slip bands, crack initiation and to determine the rate of crack propagation on the polished surface with a magnification of ×250.

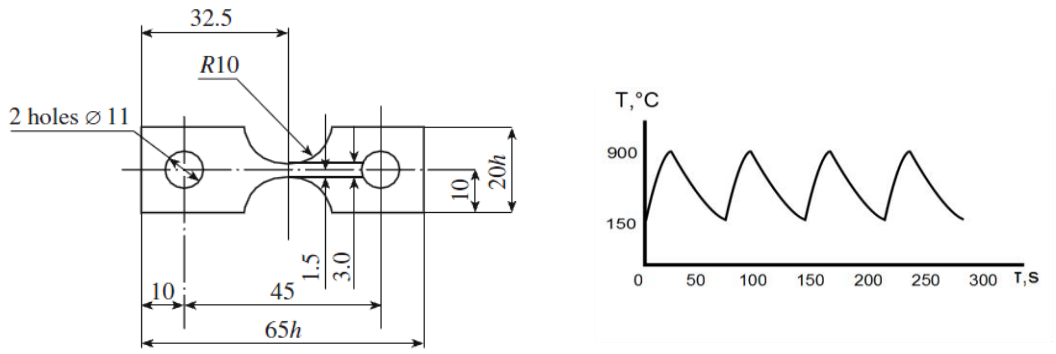

Fig. 1. The specimen for the thermal fatigue test (left) with typical temperature alteration in the middle part (right).

Tests were conducted with various values of maximum (T_{max} =900÷1100 ^{0}C) and minimum (T_{min} = 150÷700 ^{0}C) cycle temperatures. The tests with retardation time 2 and 5 minutes at T_{max} were carried out for some part of the samples. Some samples had the stress concentrator in the form of a central hole with the diameter of 0.5 mm. The test specimens had different crystallographic orientations ⟨001⟩, ⟨011⟩ and ⟨111⟩. To determine the crystallographic orientation for each sample Laue's diffraction patterns were obtained and three Euler's angles and Schmid's factors computed. Based on results of the crystallographic analysis the possible directions (angles) of the slip bands on the specimen surfaces are calculated with the aim to compare them with angles at which the samples were destroyed. Location of the fracture nucleus was determined by the results of fractographic studies using a TESCAN microscope. The comparison of experimental data on the orientation of the fracture surfaces with the results of crystallographic analysis and with the results of finite-element analysis of specimens allows to define the dependence of the failure mechanism (crystallographic or non-crystallographic) on parameters of the thermal cycle.

The results of experimental studies

The tests of mechanical properties show that the single crystal alloys have high plasticity not at all temperatures (see, for example, Table 1). Low values of plasticity δ are observed for the carbon-free alloy ZhS36 (as opposed to the carbon-alloy ZhS32) at 500 ^{0}C (as opposed to the case of high temperatures T > 900 ^{0}C).

Table 1. The mechanical properties of single crystal alloys with orientation ⟨001⟩ at 500 ^{0}C.

Alloy		$\sigma_{0,2}$, MPa	σ_F, MPa	δ, %	Ψ, %
ZhS36		964 967	982 1000	1,3 2,3	5,0 6,9
ZhS32	Schedule t/t 1	850	880	19,5	35,5
	Schedule t/t 2	810	1110	13,0	11,7

Fig. 2 shows the short-term creep curves of the alloy ZhS32. The curves obtained under stress 550 MPa at 850 ^{0}C significantly differ for various samples. Results of creep tests for the alloy ZhS36 are given in [4].

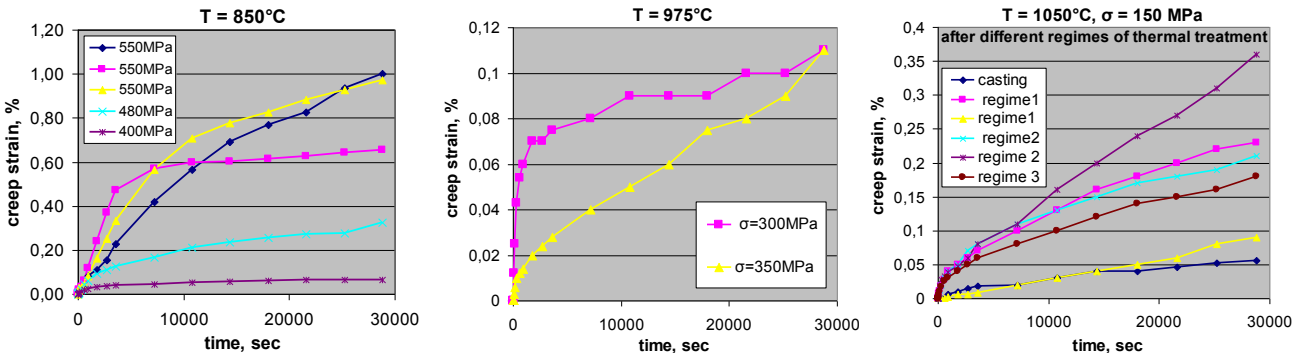

Fig. 2. Creep curves of alloy ZhS32 at 850, 975 and 1050 ^{0}C.

Tests of ZhS36 alloy show that the conditions for failure under thermal cyclic loading depend on the crystallographic orientation of single crystal alloy and also on the temperatures of cycle. Unfortunately, the experiments conducted on the alloy ZhS36 with orientations ⟨001⟩, ⟨011⟩ and ⟨111⟩ were not numerous and the obtained results reflect only a trend. However, a formulation of the failure criterion depends on the failure mode (crystallographic or non-crystallographic) [5]. In this paper, we have obtained conditions (range of thermal cycle parameters) (see Fig. 3) for fracture modes for the alloy ZhS32 with orientations close to ⟨001⟩. The accumulation of unilateral irreversible deformation (ratcheting) has been observed in all tests (see Fig. 4) for both alloys.

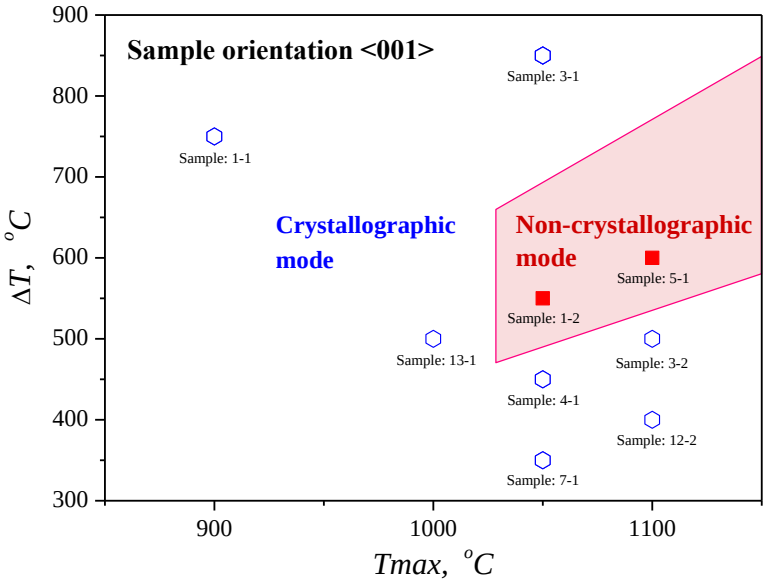

Fig. 3. Map of fracture mechanisms for the alloy ZhS32 under thermal cyclic loading.

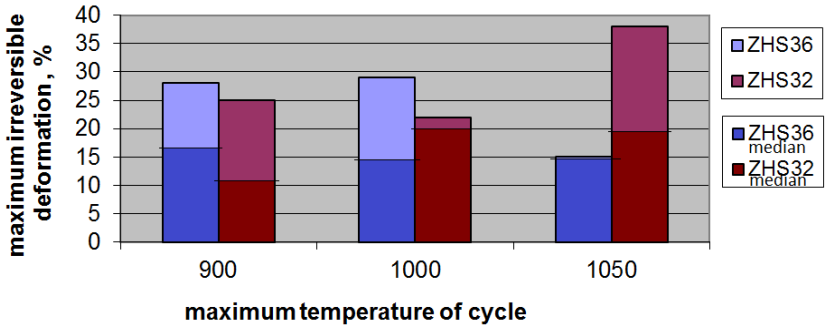

Fig. 4. Ratcheting in the alloys ZhS32 and ZhS36 under thermal cyclic loading.

Criteria of failure under static loading

The single crystal supperalloys, as a rule, are plastic materials and the possibility of brittle fracture under static loading of gas turbine blades is questionable. However, this issue requires special investigation. We consider such possibility on the basis of two (stress and deformation) failure criteria.

Effect of stress on the deformation capacity ε^* is determined by the formulas of Mahutov N.A. or Hancock J.W., Mackenzi A.C. [6]:

$$\varepsilon^* = \varepsilon_{pr} 1.7 \exp(-1.5\sigma_{mean}/\sigma_i), \quad (1)$$

$$\varepsilon^* = \varepsilon_{pr} K_e \sigma_i^2 / (3\sigma_1 \sigma_{mean}), \quad (2)$$

where ε_{pr} is maximum deformation, determined from the experiments under short-term tension, K_e is characteristic of the material state (in a brittle state $K_e = 1$, in a viscous state $K_e = 1.2$).

Effect of stress on the fracture conditions we consider in terms of the power criterion. Consider the general case of stress: $\sigma_2 = A_1\sigma_1$, $\sigma_3 = A_2\sigma_1$, where A_1 and A_2 can vary from -∞ to 1. Depending on the relations between $\sigma_1, \sigma_2, \sigma_3$ and on the ratio of $\sigma_{pr}/\sigma_{0,2}$, there is an area of brittle damage in which the tensile ultimate stress is used as a limiting strength characteristics σ_{pr} for local stresses.

The above relation can also be written in a somewhat different form. Consider the case where $\sigma_1/\sigma_i > 1$. We use an approximation of stress-strain curve in the form $\sigma_i = \sigma_{0,2} + A\varepsilon_i^{p\,m}$ and the fracture condition according to the first theory of strength $\sigma_1 = \sigma_{pr}$. Let $q = \sigma_1/\sigma_i$, then we have $q\left(\sigma_{0,2} + A\varepsilon_i^{p\,m}\right) = \sigma_{pr}$, where plastic deformation is defined by equation:

$$\varepsilon_i^p = \left[\left(\sigma_{pr}/q - \sigma_{0,2}\right)/A\right]^{\frac{1}{m}}. \quad (3)$$

Let $k = \sigma_{pr}/\sigma_{0,2}$, than $\varepsilon_i^p = \left[\left(\sigma_{0,2}k/q - \sigma_{0,2}\right)/A\right]^{\frac{1}{m}} = \left[\sigma_{0,2}\left(k/q - 1\right)/A\right]^{\frac{1}{m}}$, where $k/q > 1$. The brittle fracture takes place under $k/q = 1$.

The analysis of crack initiation in the blades under static loading (centrifugal force and bending) on the base of ***stress failure criterion*** should include:

1. Thermal finite-element analysis of the steady-state temperature field in the blade;
2. Elastic finite-element analysis of stress fields with the subsequent definition of $q = \sigma_1/\sigma_i$ and $k = \sigma_{pr}/\sigma_{0,2}$ at the corresponding temperatures for all elements of the cooled blades;
3. According to the first strength theory we accept $\sigma_{pr} = \sigma_{separation} \sim \sigma_F / (1-\psi)$ and verify the absence of equality $q = k$ at all points. For the remaining cases, we calculate the value of plastic strain by (3);
4. Estimation of strength by means of comparison ε_i^p (3) with the limiting plasticity ε^* (1) or (2).

The analysis of crack initiation in the blades under static loading (centrifugal force and bending) on the base of ***strain failure criterion*** should include:

1. Thermal finite-element analysis of the steady-state temperature field in the blade;
2. Elastoplastic finite-element analysis with the definition of zones of plastic deformation and maximum values $\varepsilon_{i\,\max}^p$ for all elements of cooled blades;
3. Comparison of the obtained value $\varepsilon_{i\,\max}^p$ with the limiting characteristic ε^* (1) or (2) at the corresponding temperatures taking into account also their decrease under the effect of aging at operating temperatures and long exposures;
4. Viscoelastic finite-element analysis of stress relaxation processes with the initial conditions obtained by elastoplastic analysis (see 2);

5. Calculate the equivalent stress. If the value of $(\sigma_0-\sigma_{res})$ / E is less than or approximately equal to the maximum ductility under creep conditions at a suitable temperature, determined by the formulas

$$p^* = \varepsilon_c 1.7 \exp(-1.5\sigma_{mean}/\sigma_i), \quad (4)$$

$$p^* = \varepsilon_c K_e \sigma_i^2 /(3\sigma_1\sigma_{mean}), \quad (5)$$

than a brittle fracture under conditions of stress relaxation is possible.
6. Accept the assumption that the microcracks are formed in the zone of inelastic deformation over time. Determine the size of the zone of inelastic deformation (plastic and creep) and compare it with the limit values corresponding to the beginning of accelerated crack growth in the non-linear fracture mechanics.

Criteria of failure under thermal cyclic loading
For the prediction of TMF failure of single crystal materials it is reasonable to use the deformation criterion proposed in [5]. The crack initiation criterion is a condition for achieving critical value of the total damage initiated by different mechanisms:

$$D_1(\Delta\varepsilon_{eq}^p) + D_2(\Delta\varepsilon_{eq}^c) + D_3(\varepsilon_{eq}^p) + D_4(\varepsilon_{eq}^c) = 1. \quad (6)$$

The criterion (6) is based on a linear summation of damages caused by cyclic plastic strain

$$D_1 = \frac{1}{C_1}\sum_{i=1}^{n}(\Delta\varepsilon_{eq_i}^p)^k, \quad (7)$$

cyclic creep strain

$$D_2 = \frac{1}{C_2}\sum_{i=1}^{n}(\Delta\varepsilon_{eq_i}^c)^m, \quad (8)$$

unilaterally accumulated plastic strain

$$D_3 = \frac{1}{\varepsilon_r^p}\max\varepsilon_{eq}^p \quad (9)$$

and unilaterally accumulated creep strain

$$D_4 = \frac{1}{\varepsilon_r^c}\max\varepsilon_{eq}^c. \quad (10)$$

The C_1, C_2, k, m, ε_r^p, ε_r^c are the material parameters depending on the temperature and on the crystallographic orientation. Usually the relations $k=2$, $m=5/4$, $C_1 = \left(\varepsilon_r^p\right)^k$, $C_2 = \left(\frac{3}{4}\varepsilon_r^c\right)^m$ are used.
The different norms of strain tensor are considered as equivalent strain for (6), among them there are: the *maximum shear strain in slip system* with normal $\mathbf{n}_{\{111\}}$ to slip plane and slip direction $\mathbf{l}_{\langle 011\rangle}$

$$\varepsilon_{eq} = \mathbf{n}_{\{111\}}\cdot\boldsymbol{\varepsilon}\cdot\mathbf{l}_{\langle 011\rangle}, \quad (11)$$

the *maximum tensile strain* (maximum eigenvalue of strain tensor)

$$\varepsilon_{eq} = \varepsilon_1 = \max\arg\{\det(\boldsymbol{\varepsilon} - \lambda\mathbf{1}) = 0\}, \quad (12)$$

the *strain intensity* von Mises

$$\varepsilon_{eq} = \sqrt{\tfrac{2}{3}\, dev\boldsymbol{\varepsilon} \cdot\cdot dev\boldsymbol{\varepsilon}} = \sqrt{\frac{2}{9}\left[\left(\varepsilon_x - \varepsilon_y\right)^2 + \left(\varepsilon_y - \varepsilon_z\right)^2 + \left(\varepsilon_z - \varepsilon_x\right)^2 + \frac{3}{2}\left(\gamma_{xy}^2 + \gamma_{yz}^2 + \gamma_{zx}^2\right)\right]}, \quad (13)$$

and the *maximum shear strain*

$$\varepsilon_{eq} = \tfrac{1}{2}\left[\varepsilon_1 - \varepsilon_3\right] = \tfrac{1}{2}\left[\max \arg\{\det\left(\boldsymbol{\varepsilon} - \lambda \mathbf{1}\right) = 0\} - \min \arg\{\det\left(\boldsymbol{\varepsilon} - \lambda \mathbf{1}\right) = 0\}\right]. \quad (14)$$

The equivalent strain (11) corresponds to the crystallographic failure mode, while equivalent strains (12)-(14) correspond to the non-crystallographic failure mode.

Results of finite-element simulation

The stress-strain analysis of single crystal samples (see Fig. 1) with a concentrator (in the form of central circular hole) or without concentrator was carried out on the base of the finite-element program PANTOCRATOR [7] with an application of "physical" models of plasticity. These material models take into account that the inelastic deformation occurs in accordance with crystal slip systems by a slip mechanism and therefore deformation is strongly sensitive to the crystallographic orientation. The elastoplastic and viscoelastoplastic material models [8, 9] with nonlinear kinematic and isotropic hardening also accounting the selfhardening on each system and the latent hardening [10] between the slip systems are used in finite element simulations. The application of viscoelastic models leads to unrealistically overestimated levels of stress.

The obtained results for inhomogeneous stress, strain and damage fields allow to find the location of critical point of specimen. The damage field is obtained by the criterion (6) on the basis of analysis of strain field evolution using the experimental data on creep and elastoplastic deformation resistance curves. The typical damage field distribution after first thermal cycle ($20^oC \rightarrow T_{max}=900^oC \rightarrow T_{min}=150^oC$) is presented in Fig. 5 for the sample 5-1 from ZhS36 with the orientation $\langle 001 \rangle$.

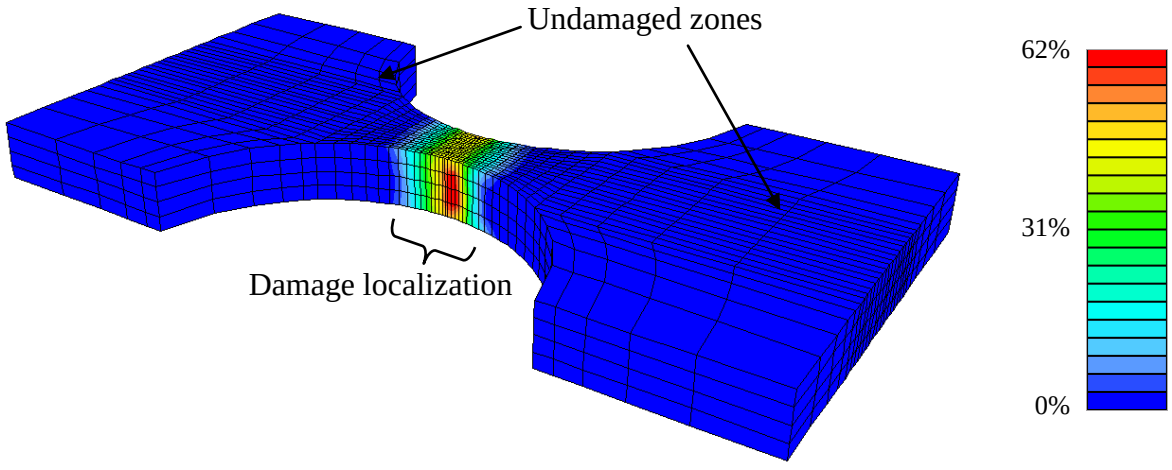

Fig. 5. Damage field distribution after first cycle for the sample 5-1 with $\langle 001 \rangle$ orientation.

The results of the finite-element simulations show that the crystallographic orientation has a significant influence on the stress-strain state of the samples (see Fig. 6), as also confirmed by the experiments [11]. The width of the hysteresis loops and the unilaterally accumulated strain are also very sensitive to thermal cyclic regime (see Fig. 7).

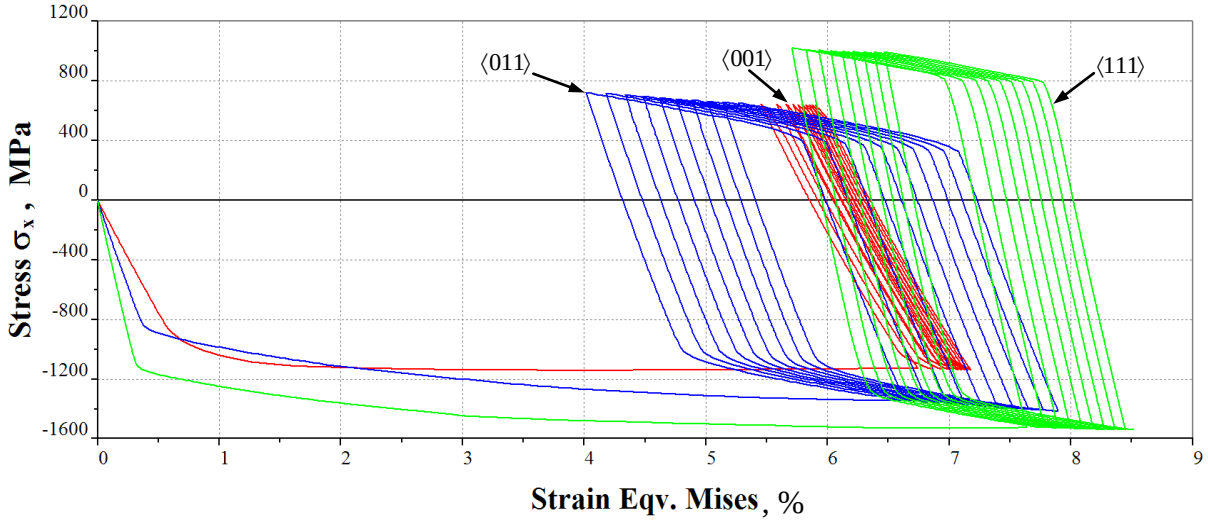

Fig. 6. Influence of crystal orientation on cyclic stress-strain curve. Results of finite-element simulations for thermal cycles with T_{max}=900°C and T_{min}=150°C (central point of specimen).

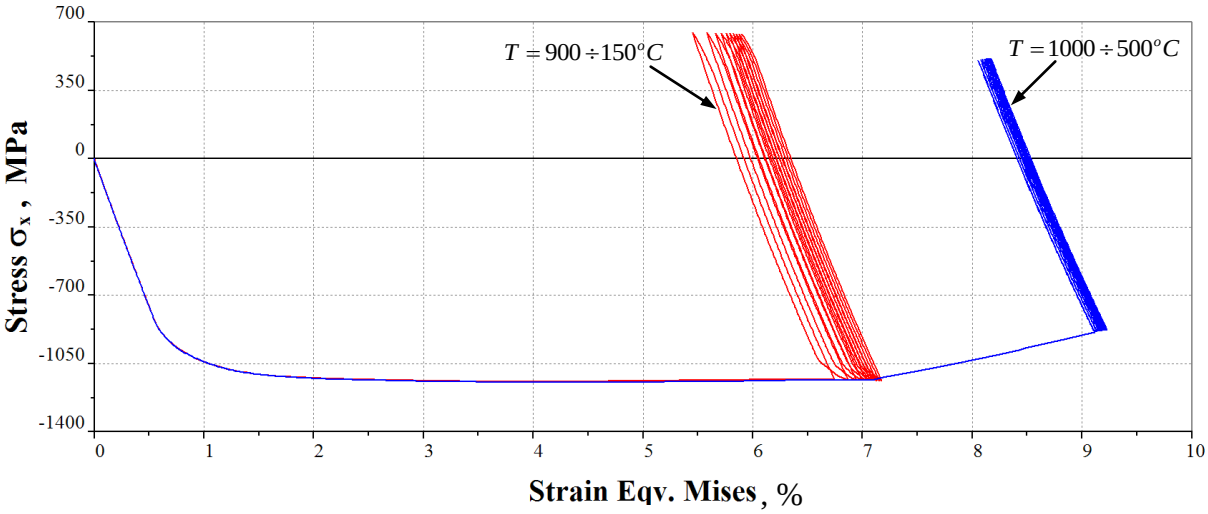

Fig. 7. Influence of temperature program on cyclic stress-strain curve. Results of finite-element simulations for specimens with ⟨001⟩ orientation (central point of specimen).

The number of cycles to crack initiation, calculated on the basis of criterion (6) using different equivalent strains (11)-(14), are given in Table 2. The satisfactory correlation is observed between criterion predictions and results of experiments (without sufficient statistical representativity).

Table 2. Deformation criterion (6) predictions vs. experimental results for the crack initiation life.

	Orien-tation	T_{max}, °C	T_{min}, °C	Number of cycles to crack initiation				
				$\varepsilon_{eq}=\varepsilon_{nl}$ (11)	$\varepsilon_{eq}=\varepsilon_1$ (12)	$\varepsilon_{eq}=\varepsilon_i$ (13)	$\varepsilon_{eq}=\gamma_{max}$ (14)	Experiment
Sample 5-1	⟨001⟩	900	150	291	238	163	237	435
Sample 5-3	⟨001⟩	1000	500	218	196	150	172	90
Sample 1-2	⟨111⟩	900	150	85	73	59	75	190
Sample 2-1	⟨011⟩	900	150	20	20	13	20	17

Conclusions

1. In the development of investigations of I.L. Svetlov, E.R. Golubovsky, of authors and of other researchers a series of tests were conducted on the definition of thermal fatigue resistance and short-term creep of single-crystal alloy ZhS32 with determination of temperature range causing changes in failure modes.
2. The failure criteria for the single crystal alloys under static and thermal cyclic loadings are proposed and discussed. The satisfactory correlation is observed between deformation criterion (6) and obtained experimental results. All considered variants of equivalent strains (11)-(14) give practically the same results. The criterion, using strain intensity von Mises (13), offers the most conservative estimation.
3. The finite element simulations of single crystal specimens under thermal cyclic loading have been performed by using different material models. The obtained results indicate an applicability of the proposed deformation criteria of failure for the single crystal alloys ZhS32 and ZhS36 for temperatures up to 1100 ^{o}C.

Acknowledgements

The study was supported by the Russian Fundamental Research Program, Project №12-08-00943. The authors are also grateful to S.M. Odabai-Fard for helping prepare the paper.

References

[1] E.N. Kablov, E.R. Golubovsky. *Heat-resistant nickel alloys*. M: Mechanical Engineering, (1998).

[2] R.E. Shalin, I.L. Svetlov, E.B. Kachanov, V.N. Toloraiya, O.S. Gavrilin. *Single crystals of nickel-base superalloys*. M: Mechanical Engineering, (1997).

[3] L.B. Getsov, N.I. Dobina, A.I. Rybnikov, A.S. Semenov, A.A. Staroselsky, N.V. Tumanov. Thermal fatigue resistance of single crystal alloy. Strength of Materials № 5 (2008), pp. 54-71.

[4] L.B. Getsov. *Materials and strength components of gas turbines*.Vol. 1 and 2. Rybinsk. Publ. House. Gas Turbine Technology, (2011).

[5] L.B. Getsov, A.S. Semenov. Failure criteria for polycrystalline and single crystal materials under thermal cyclic loading. Proc. NGO CKTI, N296. Strength of materials and resource elements of power. St. Petersburg, (2009), pp. 83-91.

[6] L.B. Getsov, B.Z. Margolin, D.G. Fedorchenko. The determination of elements of engineering safety margins in the calculation of structures by finite element method. Proc. NGO CKTI, N296, Strength of materials and resource elements of power. St. Petersburg, (2009), pp. 51-66.

[7] A.S. Semenov. PANTOCRATOR-finite-element software package, focused on the solution of nonlinear problems in mechanics. Proc. of V Int. Conf. "Scientific and technical problems of forecasting the reliability and durability of the structures and methods for their solution", St. Petersburg: Publishing House of Polytechnic University, (2003), pp. 466-480.

[8] G. Cailletaud. A Micromechanical Approach to Inelastic Behaviour of Metals. Int. J. Plast., 8 (1991), pp 55–73.

[9] J. Besson, G. Cailletaud, J.-L. Chaboche, S. Forest. *Non-linear mechanics of materials*. Springer, (2010).

[10] U.F. Kocks, T.J. Brown. Latent hardening in aluminium. Acta Metall. 14 (1966), pp. 87–98.

[11] L. Getsov, A. Semenov, A. Staroselsky. A failure criterion for single crystal superalloys during thermocyclic loading. Materials and Technology. 42 (2008), pp. 3-12.